Electrochemical preparation and physicochemical study of polymers obtained from carbazole and N-((methoxycarbonyl)methyl)carbazole

S. Lakard, E. Contal, K. Mougin, C. Magnenet, B. Lakard

Electrochemical preparation and physicochemical study of polymers obtained from carbazole and N-((methoxycarbonyl)methyl)carbazole

S. Lakard[a], E. Contal[a], K. Mougin[b], C. Magnenet[a], B. Lakard[a,*]

a Institut UTINAM, UMR CNRS 6213, Univ. Bourgogne Franche-Comté, 16 Route de Gray, 25030 Besançon, France

b Inst Sci Mat Mulhouse IS2M, UMR CNRS 7361, Univ. Haute Alsace, 15 Rue Jean Starcky, BP 2488, 68057 Mulhouse, France

* To whom correspondence should be sent: E-mail: boris.lakard@univ-fcomte.fr; Tel: + (33) 3 81 66 20 46.

Abstract

The polymerization of carbazole (Cz) and N-((methoxycarbonyl)methyl)carbazole (CzE) was carried out by electrochemical oxidation in acetonitrile solution. Different feed ratios of monomers were used to deposit polymer thin films with different compositions and study the influence of the ratio of monomers on the electrochemical, morphological, mechanical and adhesive properties of the polymer films. The electrochemical oxidation led to the deposition of a polymer film whatever the feed ratio but the thickness of the film increased with the portion of unmodified carbazole. On the contrary, the composition of the monomer mixture had a low influence on the AFM adhesion forces between the AFM tip and the polymer film. Depending on the feed monomer ratio, the morphology was either globular or columnar (when the portion of CzE was comprised between 10 and 70%). The stiffness of the polymer films was also found to be strongly dependent on the feed ratio since it varied from 2 to 115 GPa depending on the monomer ratio. The polymer films prepared from the ratios 90:10 and 70:30 in Cz:CzE monomer solutions were found to be the most interesting ones since they led to thick and conducting polymer films with a good adhesion and a low stiffness. Moreover, these coatings were uniform and exhibited an original columnar structure.

Keywords:

Conducting polymer; Carbazole; Electrodeposition; Atomic Force Microscopy; Stiffness.

1. Introduction

Conducting polymers are a class of organic materials exhibiting the electrical and optical properties of both metals and semiconductors [1]. Due to these interesting properties but also their low cost and ease of synthesis, conducting polymers have a wide range of practical applications including: light-emitting diodes [2], anti-corrosion [3], energy storage [4], chemical sensors [5] and biosensors [6], and biomedical engineering [7]. If more than 25 conducting polymer systems have already been reported, the most intensively used are those obtained from thiophene [8,9], aniline [10,11], pyrrole [12,13], fluorene [14,15] and 3,4-ethylenedioxythiophene [16,17]. Carbazole is another heterocyclic organic compound which possesses a good chemical, thermal and environmental stability and which showed potential applications in gas storage and separation, catalysis, and sensors [18]. Carbazole and its derivatives have also attracted great attention due to their electrical and optical properties [19] which make them very useful in the field of optoelectronics [20-22]. Carbazole can be chemically and electrochemically synthesized from monomers containing linked conjugates units [23-25]. The substitution of carbazoles by functional groups can be performed at the nitrogen atom [23] or at C-3 and C-6 atoms [26,27] leading to a wide variety of functional groups. The introduction of such groups allows to improve the polycarbazole solubility and tune its optical and electrical properties. Besides, numerous efforts have been done to prepare polymers combining carbazole units with other units to improve their properties. For example, pyrrole and carbazole led to a polymer presenting a higher conductivity than polycarbazole [28]. 9-ethylcarbazole and 3-hexylalkylthiophene were also polymerized, leading to a conjugated film with a higher thermal stability than polyhexylthiophene [29]. Also, the electrochemical oxidation of 2,7'-carbazole and 3-octylthiophene monomers led to a polymer presenting a very regular structure and both n- and p-doping/undoping processes

[30]. Other polymers were obtained from carbazoles and s-triazines leading to superstructural conducting polymers with high optical contrast and high thermal and electrochemical stability [31,32]. Similarly, polymers synthesized from carbazole and phenazine derivatives showed various structures leading to optical devices with very different photodetectivity performances [33]. Besides, a polymer built from a fluorene and a carbazole, with an alkyl functional group at the 9-position, demonstrated excellent thermal stability and good optical performance since high efficient blue light-emitting properties were obtained [34].

From this literature [26,27,31-34], it is noticeable that polymers and copolymers based on carbazole and its derivatives have been mainly used for applications in optoelectronics due to their intrinsic properties. Another possible application for carbazole-based materials, taking advantage of their conductivity and easiness to functionalize them, concerns (bio)sensors. But, until now, only a few studies have been dedicated to this topic. Among these works, several were dedicated to the development of fluorescent sensors based on carbazole derivatives and used to detect cyanide anions [35], SO_2 derivatives [36], mercury (II) ions [37] or copper (II) ions [38]. Two electrochemical biosensors based on amperometric detection were also developed. The first one was an electrochemical glucose biosensor based on an alkylcarbazole and a zinc(II) phthalocyanine [39] when the second one was an electrochemical tyrosinase biosensor based on a dicarbazole derivative functionalized by an *N*-hydroxysuccinimide group [40]. Also, Perie *et al.* functionalized N-alkylcarbazoles and introduced ester groups in the polycarbazole backbone to prepare polymers suitable for covalent grafting of proteins, as demonstrated for bovine serum albumin protein [41].

If polycarbazole films have interesting optical and electrical properties, documented in the literature [21-24,26-34], it is frequently necessary to functionalize them to introduce

chemical groups improving the mechanical strength or chemical reactivity of the polymer films. One drawback of these electrodeposited films, when incorporated in devices or sensors, is their mechanical stability and stiffness. So, in this paper, we made the choice to deposit polymer films by electrochemical oxidation of carbazole (Cz) and N-((methoxycarbonyl)methyl)carbazole (CzE) monomers in an attempt to prepare thin films with enhanced mechanical stability. Indeed, it was expected that the introduction of the ester groups within the polymer film could allow an improvement of its mechanical properties (since such groups are often incorporated in the formulation of plasticizers, resins and lacquers) and could open the way to applications in biology or biosensors field since ester groups are involved in enzyme reactions and serve as protecting group for an alcohol or a carboxylic acid function during a peptide synthesis. Consequently, the present paper reports on the electrochemical oxidation of solutions composed of carbazole and N-((methoxycarbonyl)methyl)carbazole monomers using different ratios of Cz and CzE monomers. Then, the physicochemical properties of the polymer films were investigated as well as the influence of the portion of each monomer.

2. Experimental

2.1. Materials and reagents

Carbazole (>95%) was purchased from Sigma Aldrich. Lithium perchlorate (>95%) was also from Sigma Aldrich and used as supporting salt for electrochemical experiments. Acetonitrile (>99.5 %) was purchased from Fisher Scientific and used as solvent for electrochemical experiments. All the chemical reagents used to synthesize N-((methoxycarbonyl)methyl) carbazole were from Sigma Aldrich. The synthesis protocol of N-((methoxycarbonyl)methyl) carbazole is not reported here since it has been previously described in detail [42].

Rectangular-shaped FTO (Fluorine-doped Tin Oxide) coated glass substrates (10 mm x 30 mm, thickness: 1.1 mm, R = 80 Ω/square) were purchased from Solems.

2.2. Electrochemical deposition of polymer films

Electrochemical experiments were conducted at room temperature in a conventional three-compartment electrochemical cell using a platinum wire (0.785 mm^2) or a FTO coated glass substrate as the working electrode, a Saturated Calomel Electrode (SCE) as the reference electrode and a Pt sheet as the auxiliary electrode. Electrolytic solutions with the following molar ratios of Cz to CzE (Cz:CzE) were prepared: 95:5, 90:10, 70:30, 50:50, 30:70 and 5:95. For example, to prepare an electrolyte with a Cz:CzE ratio of 90:10 (leading by electrochemical oxidation to a polymer film denoted Cz_{90}-CzE_{10}), 18 mL of Cz (10^{-2} M) and 2 mL of CzE (10^{-2} M) were added to an acetonitrile solution with 0.1 M lithium perchlorate. All electrochemical measurements (cyclic voltammograms and chronoamperometries) were carried out at room temperature with a VersaSTAT MC potentiostat/galvanostat from Princeton Applied Research.

2.3. Characterization techniques and numerical calculations

AFM microscopy. Atomic Force Microscopy (AFM) was used to investigate the morphological, adhesive and mechanical properties of electrodeposited thin films. The physico-chemical and mechanical nanoscale features of the samples were measured using a Bruker Multimode 8 AFM with the Peakforce Quantitative Nanomechanics (PeakForce QNM) mode. PeakForce QNM mode is a recent advancement in AFM method providing quantitative nanomechanical mapping mode with the simultaneous measurement of the sample's adhesion between tip and sample surface, Young's modulus (according to either

DMT or Sneddon model), deformation and energy dissipation along with the surface topography. The imaging scan size was (5 μm x 5 μm). The average adhesion and the DMT Modulus were determined using the Gwydion software. QNM etched silicon probes (RTESPA-300 probes presenting a nominal spring constant k ≈ 40 N/m) were provided by Bruker. All used tips were calibrated according to Bruker's recommendations. The results were analysed by both Nanoscope analysis 1.9 software provided by Bruker and Gwyddion. The adhesion and DMT modulus parameters were measured for at least three representative AFM images from different areas of each bead, and at least three different samples for each film were studied.

SEM microscopy. The topography of the polymer films was investigated, without prior metallization, using a high-resolution SEM microscope Quanta 450W from FEI. The electron beam energy used was 12.5 keV and the working distance used was 10 mm.

Ab initio calculations. The structure and electronic states of Cz monomers (Fig. 1a), CzE monomers (Fig. 1b) and Cz-CzE dimers were determined by *ab initio* quantum chemical calculations. In particular, the free energy in solvent of these molecules was calculated and used as a criterion of stability. These calculations were performed with the GAMESS (General Atomic and Molecular Electronic Structure System) open-sourced software package developed in Iowa State University. Density Functional Theory was used since it is particularly appropriate to model π-conjugation systems due to the inclusion of electron correlation effects [43-45]. So, after an initial optimization of the starting geometries using the semi-empirical PM3 approach [46], the calculations were performed with the B3LYP method (combined with a 6-31G* basis set) which is a DFT method involving the gradient correction of the exchange functional by Becke [47] and the Lee-Yang-Parr correction functional [48]. Besides, the Polarizable Continuum Model (PCM), which is a commonly used

method in computational chemistry to model solvation effects providing a realistic description of molecular shape by constructing the solute cavity from a union of atom-centered spheres, was employed to calculate the total free energy of the carbazoles in acetonitrile (in hartrees, with 1 hartree = 627.51 kcal/mol).

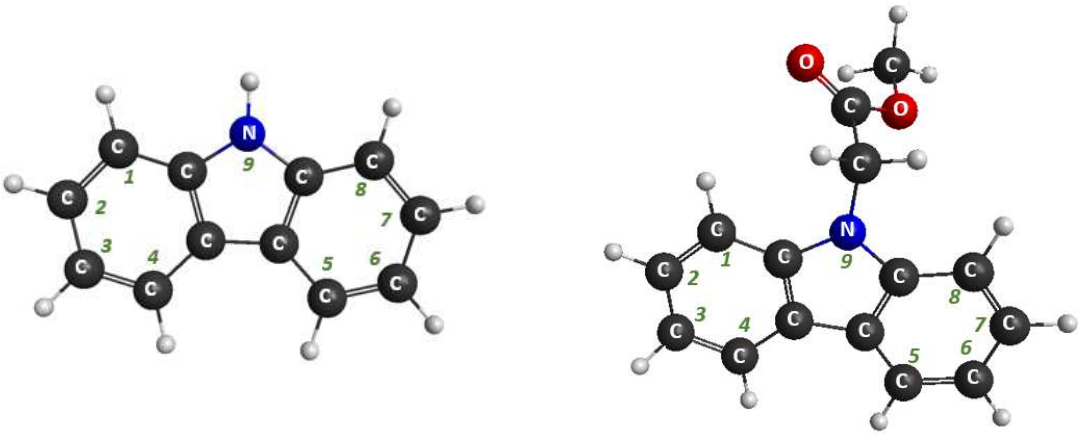

(a) (b)

Figure 1: Structure of carbazole (a) and N-((methoxycarbonyl)methyl)carbazole (b).

3. Results and Discussion

3.1. Electropolymerization of carbazole (Cz) and N-((methoxycarbonyl)methyl)carbazole (CzE):

- Electropolymerization of carbazole:

The oxidation of 10^{-2} M carbazole was achieved by potentiodynamic polymerization at a platinum electrode by applying 5 potential sweeps between 0 and +2 V/SCE, with a scan rate of 50 mV/s, in an acetonitrile solution containing 0.1 M $LiClO_4$ (Fig. 2a). The onset oxidation potentials of carbazole, leading to radical cations, appeared at +1.05 V/SCE. After the first scan, the intensity of the peak corresponding to the oxidation of Cz monomers increased with repeated scans and shifted towards higher values. Moreover, the redox process of

polycarbazole (PCz) took place since the oxidation and reduction peaks of polycarbazoles were clearly visible from the second potential scan at +0.8 and +0.75 V/SCE, respectively. Indeed, the presence of these redox peaks clearly indicate that the film is electroactive since the oxidation peak at +0.8 V/SCE is associated with the oxidation of PCz and the insertion of counter-anions into the polymer film, and the reduction peak at +0.75 V/SCE with the reduction of PCz and the ejection of counter-anions from the polymer film. Besides, the film deposited from the oxidation of Cz monomers was thick and dark green-coloured to the eye when prepared at a FTO electrode (Fig. 3) by applying a potential of + 1.5V/SCE during 3 min. As can be seen in the AFM image (Fig. 2b), the morphology of the deposited film was globular (the size of the globules being comprised between 500 nm and 2 µm) and the maximum height was 0.97 µm. The AFM force adhesion between the polymer film and the AFM tip was also measured leading to an average value of 20 ± 5 nN when the Young modulus of the polymer film was estimated to 64 GPa from AFM measurements. This high Young modulus indicates that the electrodeposited polycarbazole film has a high stiffness which could be responsible from the cracks observed in the SEM image (Fig. 2c). These experiments evidence that conducting polycarbazole films can be obtained by electro-oxidation of carbazole but the presence of numerous cracks shows that mechanical properties of the resulting film are not good enough and must be improved.

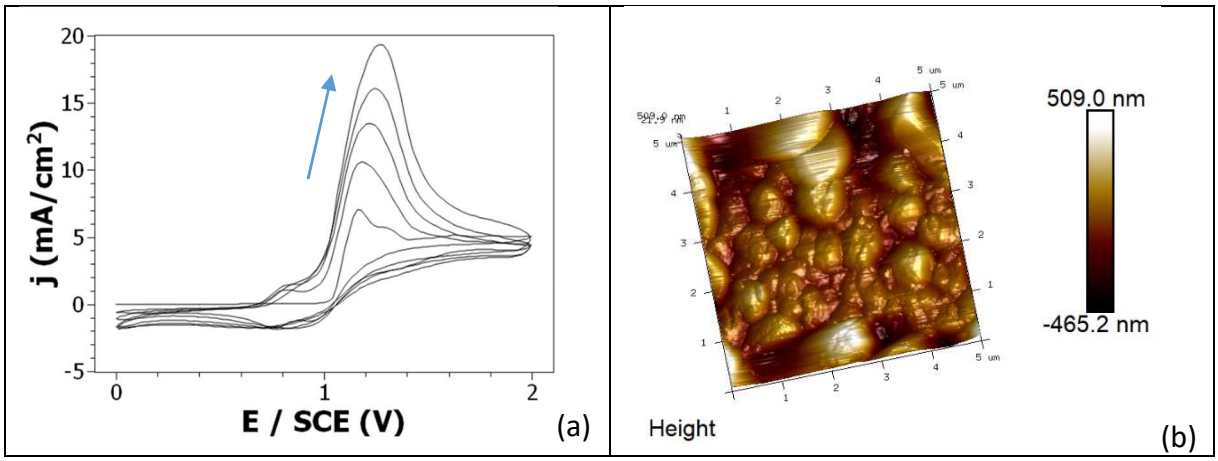

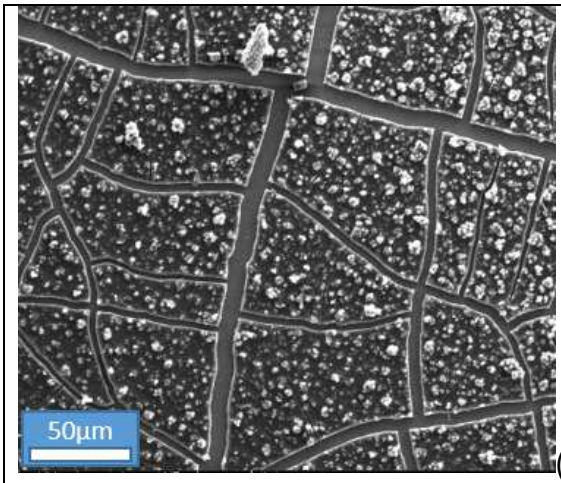

(c)

Figure 2: Cyclic voltammetry of 10^{-2} M Cz in 0.1 M $LiClO_4$/ACN at a Pt electrode with a scan rate of 50 mV/s (a). AFM (b) and SEM (c) images of the PCz film.

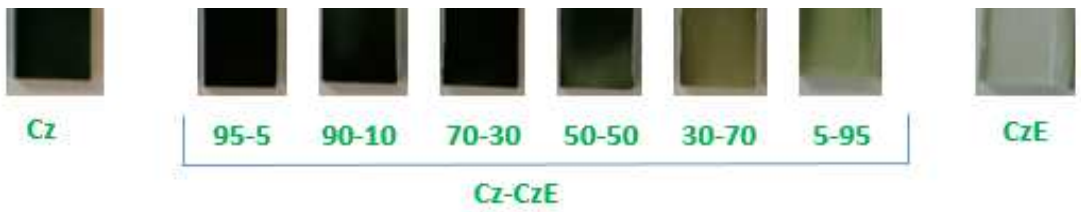

Figure 3: Photographs of polymer films deposited by oxidation of Cz, CzE and Cz:CzE solutions.

- Electropolymerization of N-((methoxycarbonyl)methyl)carbazole:

In an attempt to improve the mechanical properties of polycarbazole films, the electrochemical oxidation of a carbazole modified with an ester group was performed. Thus, the oxidation of 10^{-2} M N-((methoxycarbonyl)methyl)carbazole was carried out in the same conditions as for carbazole. The onset oxidation potentials of CzE appeared at +1.1 V/SCE (Fig. 4a). This oxidation potential is slightly higher than the one observed during the oxidation of Cz. On the contrary, the shape of the cyclic voltammogram was different since the increase of the oxidation peak intensity with repeated scans was strongly lower, indicating a poor electroactivity of the formed film, as well as the shift towards higher

values. The poor electroactivity of the film is also confirmed by the absence of redox peaks at +0.7-0.8 V/SCE which could have been associated with the insertion (resp. ejection) of counter-anions into (resp. from) the polymer film. Moreover, no additional oxidation peak that could be attributed to the polymer (PCzE) resulting from the oxidation of CzE was clearly visible indicating that the polymerization process is more difficult than the one of Cz into PCz. This was confirmed by the picture of the film since only a very thin film was visible to the eye at the FTO electrode when prepared at a FTO electrode by applying a potential of + 1.5V/SCE during 3 min (Fig. 3). The morphology of the electrodeposited film was globular (Fig. 4b) but the size of the globules was lower for PCzE (< 500 nm) than for PCz films (500-2000 nm) as well as the maximum height (0.09 µm compared to 0.97 µm) indicating that PCzE film is strongly thinner than PCz film. On the contrary, the AFM force adhesion of both polymer film was similar since it reached 15 ± 5 nN for PCzE (compared to 20 ± 5 Nn for PCz). Besides, the Young modulus of the PCzE film was evaluated to 161 GPa indicating that the stiffness of the PCzE polymer film was even higher than the one of PCz film. Consequently, replacing PCz by PCzE didn't allow to reduce the stiffness of the film and to improve its mechanical properties.

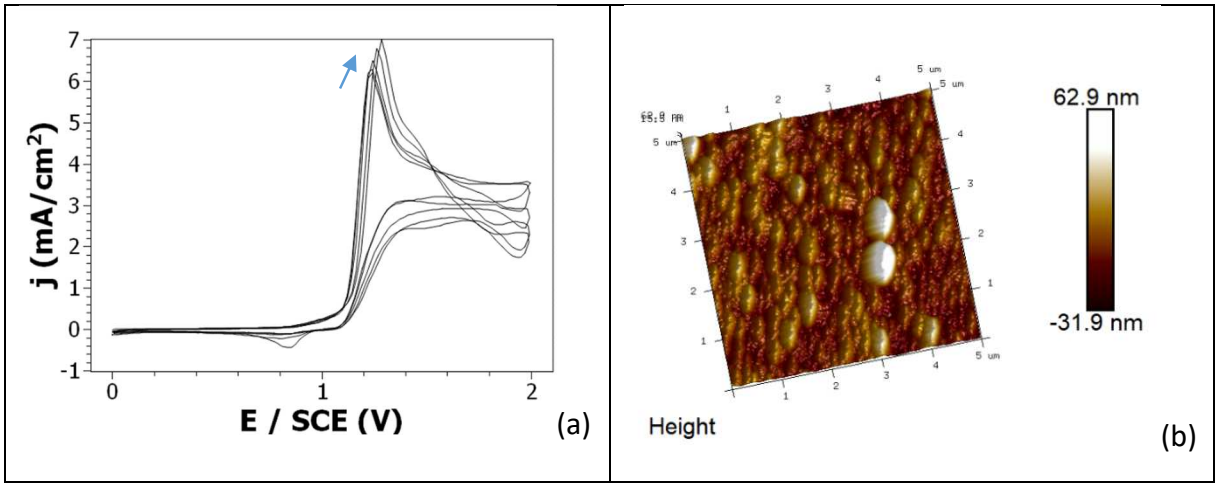

Figure 4: Cyclic voltammetry of 10^{-2} M CzE in 0.1 M $LiClO_4$/ACN at a Pt electrode with a

scan rate of 50 mV/s (a). AFM image of the PCzE film (b).

- *Gibbs free energy of activation of Cz and CzE:*

The cyclic voltammogramms previously obtained (Fig. 2a and 4a) evidenced that the oxidation of Cz is easier than the oxidation of CzE since the onset oxidation potential of Cz (+ 1.05 V/SCE) is lower than the one of CzE (+ 1.10 V/SCE). Moreover, the deposited film is clearly thicker in the case of Cz (Fig. 3). To understand these differences, the free energy in solvent of Cz and CzE monomers (denoted G_{Cz} and G_{CzE}, respectively) as well as the free energy in solvent of their corresponding radical cations (denoted $G_{Cz}^{+\circ}$ and $G_{CzE}^{+\circ}$) were calculated using *ab initio* calculations. These calculations allow to access the Gibbs free energy of activation ($\Delta G_X^{\neq} = G_X^{+\circ} - G_X$) of the oxidation reactions leading from monomers to radical cations. Thus, the Gibbs free energy of activation leading from CzE to its radical cation ($\Delta G_{CzE}^{\neq} = G_{CzE}^{+\circ} - G_{CzE}$ = -783.971 - (-754.176) = + 0.205 hartrees) is higher than the one leading from Cz to its radical cation ($\Delta G_{Cz} = G_{Cz}^{+\circ} - G_{Cz}$ = -516.950 - (-517.150) = + 0.200 hartrees) by 0.005 hartrees which correspond to 13.1 kJ/mol. So, these calculations confirm electrochemical experiments since they evidence that the oxidation of CzE is energetically less favourable that the oxidation of Cz.

3.2. Electropolymerization of mixtures of Cz and CzE:

3.2.1. Polymers with a high portion of Cz monomers:

- *Electrochemical oxidation:*

Since the oxidation of both Cz and CzE molecules lead to the formation of a thin polymer film with a high stiffness, a solution to electrodeposit films with improved mechanical properties

could be the polymerization of Cz and CzE monomers. In a first time, the oxidation of electrolytic solutions with the Cz:CzE ratios of 95:5, 90:10 and 70:30 was performed in 0.1 M $LiClO_4$ / acetonitrile solution and the resulting cyclic voltammetries were used to analyze the polymerization process. Thus, the CVs recorded for these three Cz:CzE ratios were very similar and exhibited during the first scan a strong anodic peak whose maximum current density was located at +1.2-1.3 V/SCE (Fig. 5). During the following scans, the electrochemical polymerization continued to take place at the platinum electrode since the current density increased with repeated potential scans. Also, an anodic and a cathodic peak due to the redox process and to the insertion and desinsertion of counter-anions taking place in the polymer film were visible in the three CVs in the 0.8-0.9 V/SCE potential range, indicating a good electroactivity of the polymer films. Besides, a dark green thick solid film (characteristic of the formation of a polycarbazole film) can be observed onto the platinum electrode at the end of the cyclic voltammetry or onto the FTO electrode at the end of the chronoamperometry for these three Cz:CzE ratios (Fig. 3). So, the electrochemical behaviour obtained with these ratios was similar to the one obtained with Cz.

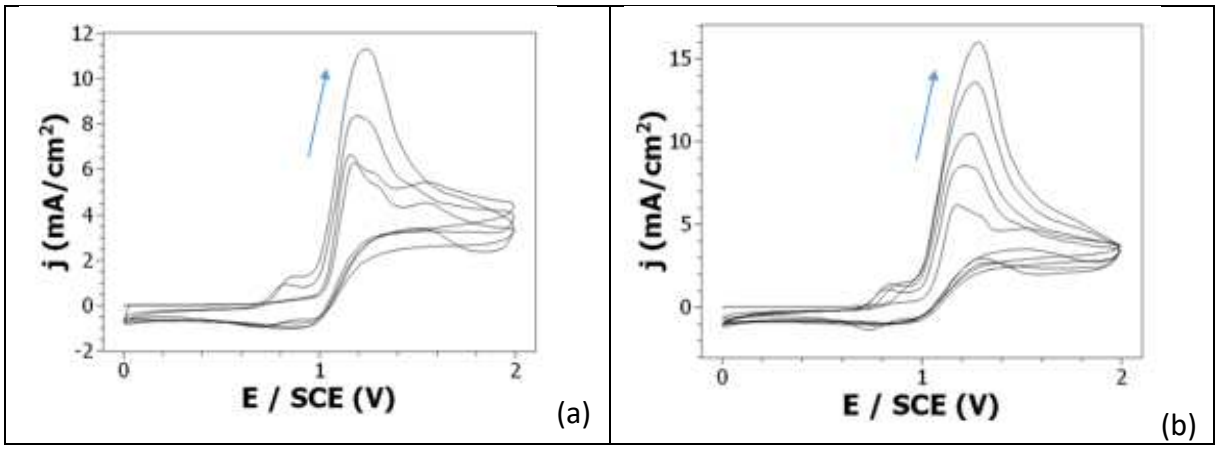

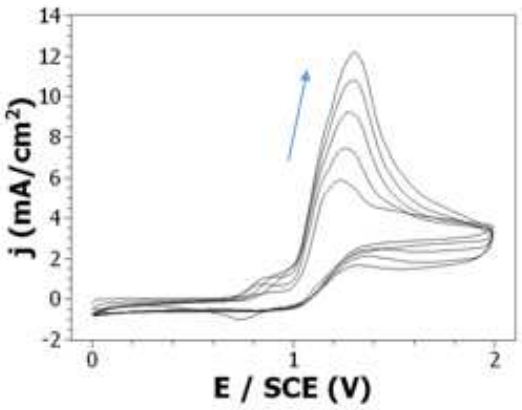

Figure 5: Cyclic voltammograms at a Pt electrode obtained in a: (a) Cz:CzE 95:5, (b) Cz:CzE 90:10, (c) Cz:CzE 70:30 acetonitrile + 0.1 M $LiClO_4$ solution. Scan rate of 50 mV/s.

- *Coupling between oxidized monomers:*

The growth mechanism leading from carbazole to polycarbazole through electrochemical oxidation has been deeply studied since the first significant works from Ambrose *et al.* [43]. It is now well-known that the oxidation of Cz results in the formation of an unstable cation radical which tends to couple with another cation radical to form a more stable bicarbazyl. The dimer produced by this one-electron reaction can be either 3,3'-bicarbazyl, the main product, or 9,9'-bicarbazyl, the minor product. Then, the oxidation of this dimer takes place and the polymer chain grows progressively to form a solid film at the electrode surface. The electro-oxidation of 9-substituted carbazoles, such as CzE, occurs in a similar way to carbazole even if only 3,3'-bicarbazyl products are formed since 9-position is already occupied [49-51].

Consequently, it could be supposed that the oxidation of a mixture of Cz and CzE monomers would result in a coupling between Cz and CzE at the 3-3' positions. To confirm this assumption the free energy in solvent ($G_{Cz\text{-}CzE}$) of the different dimers that can be obtained by coupling between the 1, 3 and 9 positions of Cz and the 1 and 3 positions of CzE (the 9-position being already occupied) was calculated using B3LYP DFT technique with 6-31G*

basis set and PCM model which allows to take the solvent into account in the calculations. As shown in Table 1, the calculations demonstrated that the most stable dimer was obtained through coupling at the 3-3’ positions (this coupling led to the lowest free energy of -1300.151 hartrees). Besides, since the dimerization takes place according to a 3-3’ coupling, it is very likely that the growth of the polymer film continues through 3-3’ coupling. So, these calculations support our assumption based on the experimental studies of the literature [43]. It also confirms that such calculations can be used as a predicting tool to determine the stability and reactivity of such reactions. Figure 6 gathers the optimized chemical structure, 3D orbitals representation and 3D electron density cartography of this 3-3’ Cz-CzE dimer. These representations evidence that such dimer is firmly delocalized all over its π system. For comparison the free energy corresponding to the coupling between 2 Cz monomers is -1033.630 hartrees and the free energy corresponding to the coupling between 2 CzE monomers is -1567.703 hartrees.

Table 1: Total free energy in solvent (in hartrees) of the different dimers that can be formed by coupling between Cz and CzE monomers.

Coupling leading to a dimer (Cz-CzE coupling)	$G_{Cz\text{-}CzE}$ (in hartrees)
9-3’ coupling	-1300.128
9-1’ coupling	-1300.135
1-1’ coupling	-1300.138
3-1’ coupling	-1300.147
1-3’ coupling	-1300.149
3-3’ coupling	-1300.151

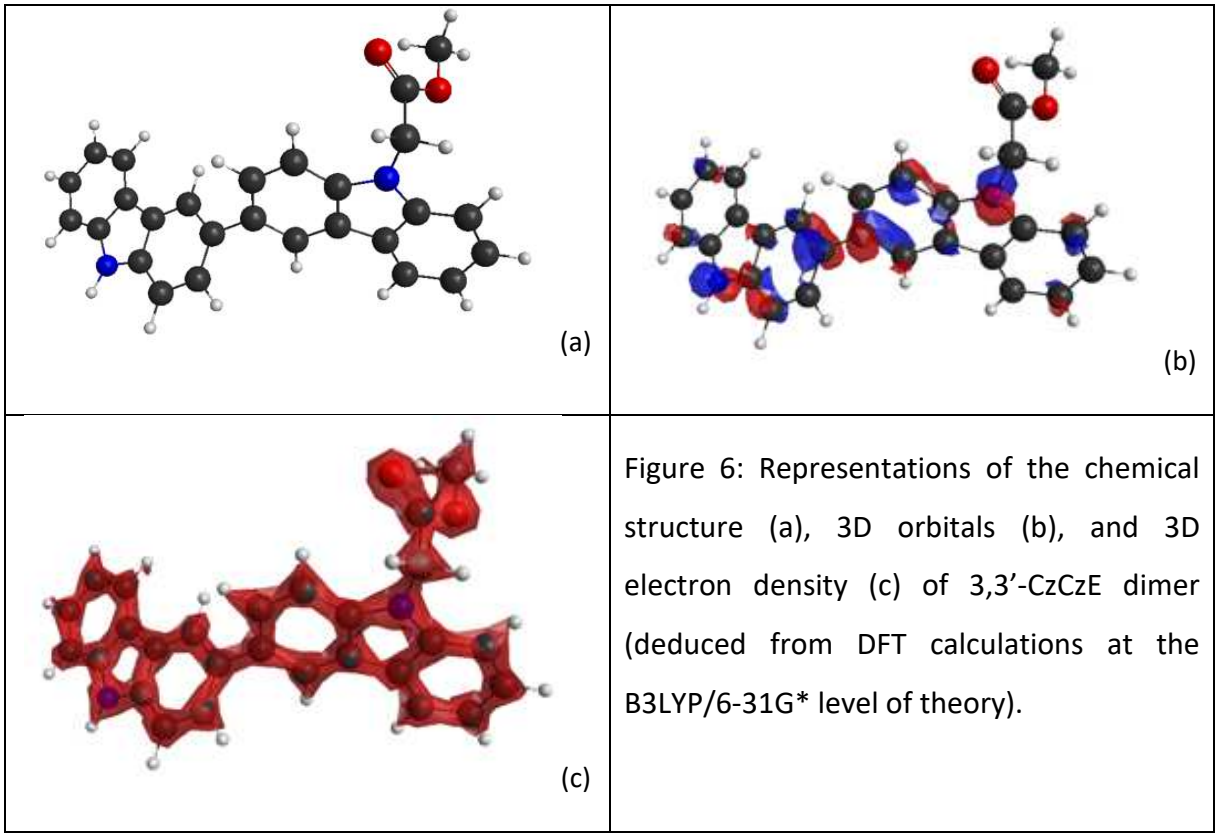

Figure 6: Representations of the chemical structure (a), 3D orbitals (b), and 3D electron density (c) of 3,3'-CzCzE dimer (deduced from DFT calculations at the B3LYP/6-31G* level of theory).

- *Physico-chemical properties:*

Atomic Force Microscopy was used to obtain information about the topography, adhesion and Young modulus of the deposited polymer films. The topography of the samples was strongly dependent on the molar ratio of Cz to CzE. Indeed, for a Cz:CzE ratio of 95:5 the polymer film morphology consists in micrometric clusters formed by aggregation of granular nodules (Fig. 7a), and so looks similar to an electrodeposited polycarbazole film (Fig. 2b). For a Cz:CzE ratio of 90:10 the morphology is quite different since it consists in columnar structures above which grains can be observed (Fig. 7c). Similar columnar structures are also observed for a Cz:CzE ratio of 70:30 but for this sample the grains are no longer visible (Fig. 7e). From these images, the maximum height of PCz, Cz_{95}-CzE_5, Cz_{90}-CzE_{10} and Cz_{70}-CzE_{30} films are: 0.98, 1.08, 1.29 and 1.19 µm, respectively. The higher thickness of Cz_{90}-CzE_{10} and Cz_{70}-CzE_{30} is probably not due to a higher amount of polymer deposited on the substrate

since the quantity of charge measured during the deposition of the film, which is known to be linked to the amount deposited through the Faraday's law, is very similar whatever the composition of the electrolyte (for Cz: 292 mC/cm^2, for Cz_{95}-CzE_5: 272 mC/cm^2, for Cz_{90}-CzE_{10}: 263 mC/cm^2, and for Cz_{70}-CzE_{30}: 259 mC/cm^2). These thickness differences are more probably due to the columnar structures of the Cz_{90}-CzE_{10} and Cz_{70}-CzE_{30} films which are more vertically oriented than the globular structure of the PCz and Cz_{95}-CzE_5 films.

The AFM force adhesion between the polymer film and the AFM tip was also measured but no clear tendency and no strong variation was observed since the average value of the adhesion of the different polymer films was 8 ± 3 nN for Cz_{70}-CzE_{30}, 12 ± 3 nN for Cz_{95}-CzE_5 and 14 ± 6 nN for Cz_{90}-CzE_{10} (Fig. 7b-d-f). These values are not far from the one obtained for PCz (20 ± 5 nN). On the contrary, the Young modulus varies significantly from PCz film to polymer films. Indeed, if the Young modulus of the PCz polymer film was estimated to 64 GPa from AFM measurements, it decreases to 29 GPa for Cz_{95}-CzE_5, to 6 GPa for Cz_{90}-CzE_{10}, and even to 2 GPa for Cz_{70}-CzE_{30} (Suppl. File 1). Such decrease of the Young modulus is really interesting since it was shown that the high stiffness of the PCz films is probably responsible from the cracks observed in the SEM image of PCz (Fig. 2c). To confirm that such cracks are due to the stiffness of the film SEM images of the polymer films have been performed (Fig. 8). Fig. 8a shows that some cracks are also present for Cz_{95}-CzE_5 polymer films even if they are less numerous and smaller than for PCz film. Besides, Fig. 8b and 8c don't exhibit any crack, thus confirming that the polymer films with the lowest Young modulus and lowest stiffness are the most homogeneous ones and possess the best mechanical properties. From these experiments, it can be concluded that Cz_{90}-CzE_{10} and Cz_{70}-CzE_{30} polymer films are the most interesting polymer films since they are thick, green-coloured, homogeneous, possess an original columnar structure and a good adhesion. Consequently, these two polymer films

have properties which could be employed for applications requiring the use of a conducting film containing ester groups and possessing good mechanical properties. They could for example be used in the future as sensitive layers of chemical biosensors based on electrochemical detection and therefore be used in the biomedical field.

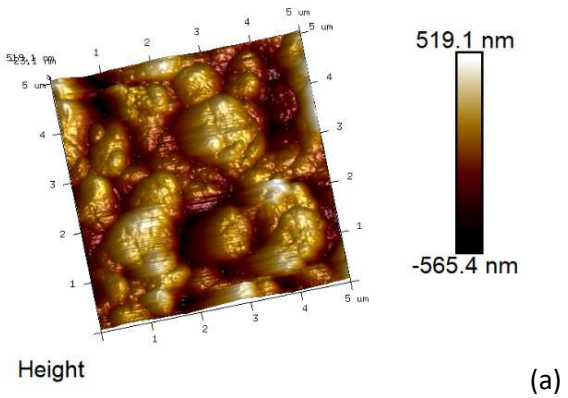

(a)

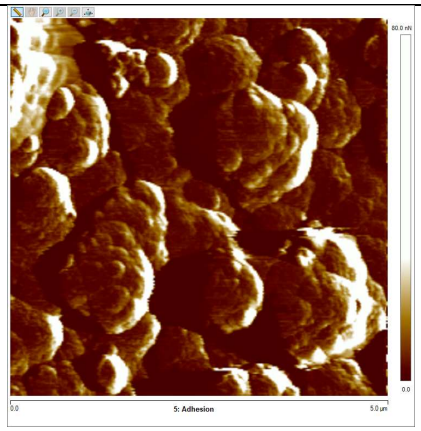

(b)

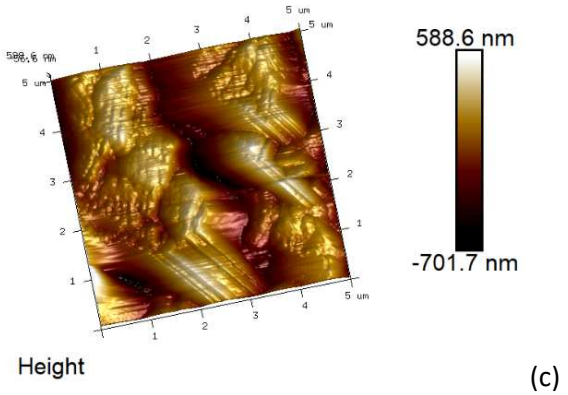

(c)

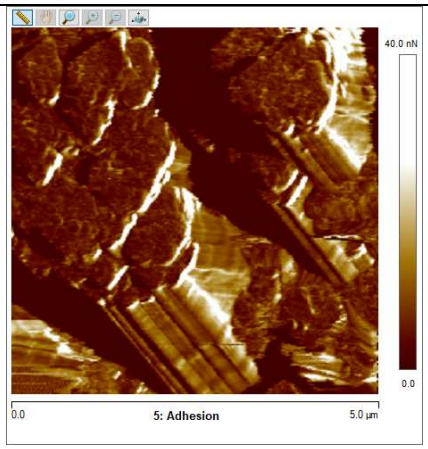

(d)

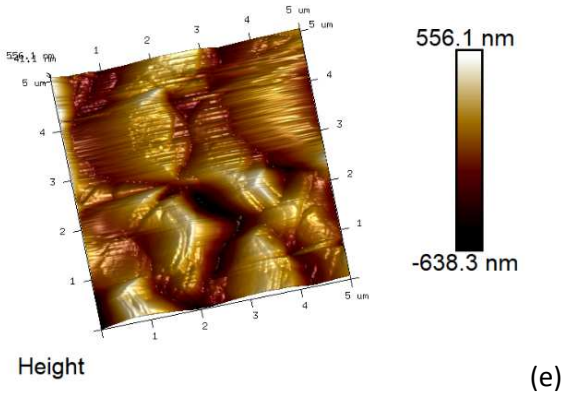

(e)

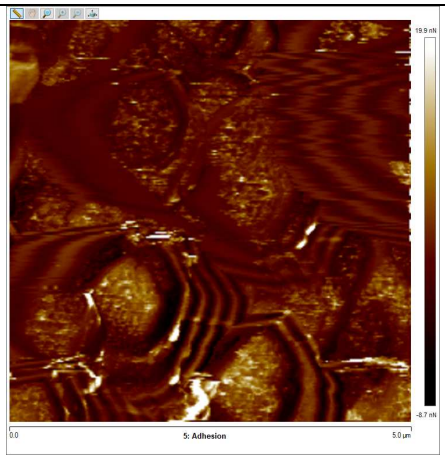

(f)

Figure 7: AFM topography (a,c,e) and adhesion images (b,d,f) of: Cz_{95}-CzE_5 (a,b), Cz_{90}-CzE_{10} (c,d), and Cz_{70}-CzE_{30} (e,f) films.

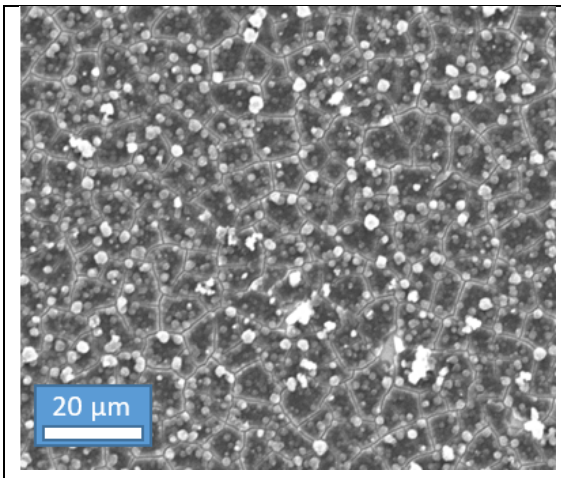

(a)

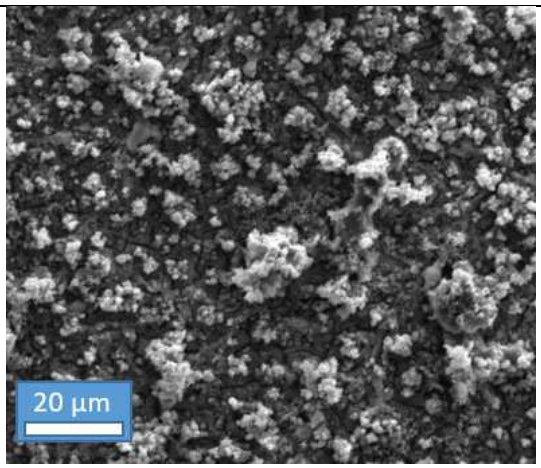

(b)

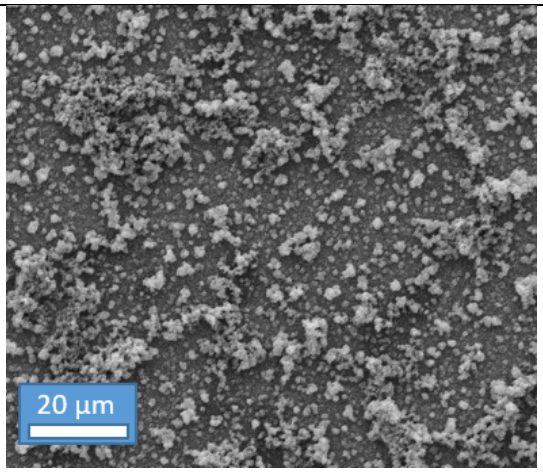

(c)

Figure 8: SEM pictures of: Cz_{95}-CzE_5 (a), Cz_{90}-CzE_{10} (b), and Cz_{70}-CzE_{30} (c) films.

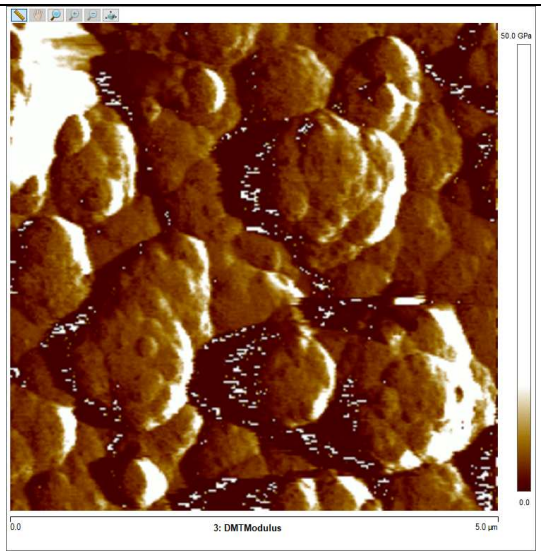

(a)

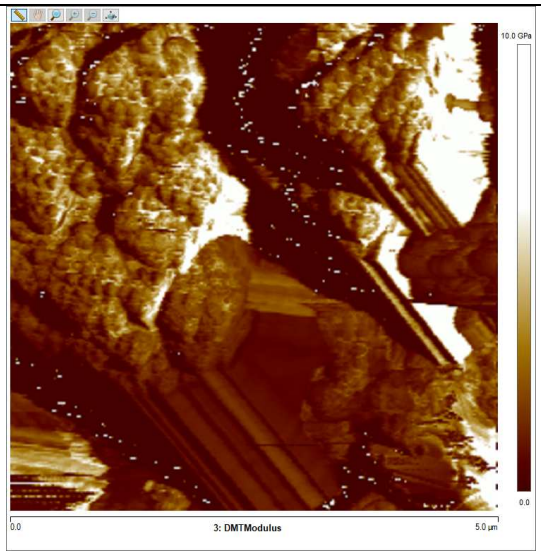

(b)

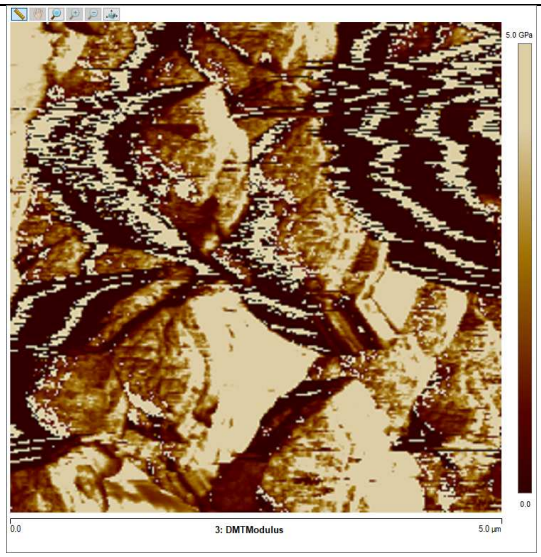

(c)

Supplementary File 1: AFM Young modulus measurements of: Cz_{95}-CzE_5 (a), Cz_{90}-CzE_{10} (b), and Cz_{70}-CzE_{30} (c) films.

3.2.2. Polymers with a low portion of Cz monomers:

- *Electrochemical oxidation:*

In a second time, the oxidation of electrolytic solutions with the Cz:CzE ratios of 50:50, 30:70 and 5:95 was carried out in 0.1 M $LiClO_4$ / acetonitrile solution. The CVs recorded for the 50:50 and 30:70 Cz:CzE ratios were quite similar to the ones obtained previously with electrolytic solutions containing a higher Cz portion. Indeed, for both ratios, the onset oxidation potentials of the mixture appeared at +1.05 V/SCE (Fig. 9). After the first scan, the

oxidation potential shifted towards higher values and the oxidation potential peak intensity increased indicating a progressive deposition of a conducting polymer at the platinum electrode. On the contrary, if the oxidation of the 5:95 Cz:CzE mixture also led to a strong oxidation peak, there was no increase of the oxidation peak intensity with repeated scans and no shift towards higher potential values indicating that this polymer film was not electroactive. So, this CV is more similar to the one obtained during the oxidation of CzE indicating that the polymerization process is difficult when a high portion of CzE is present in the electrolytic solution. This is confirmed by the picture of the deposited film which seems thinner than the other ones deposited with other ratios (containing more Cz and less CzE monomers) and whose colour is light green and not dark green as the other polymer coatings (Fig. 3).

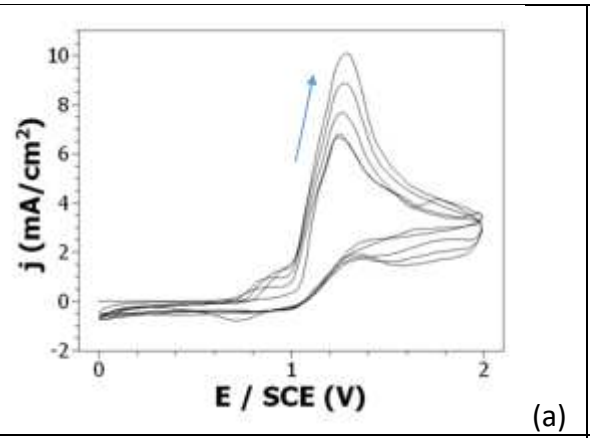

(a)

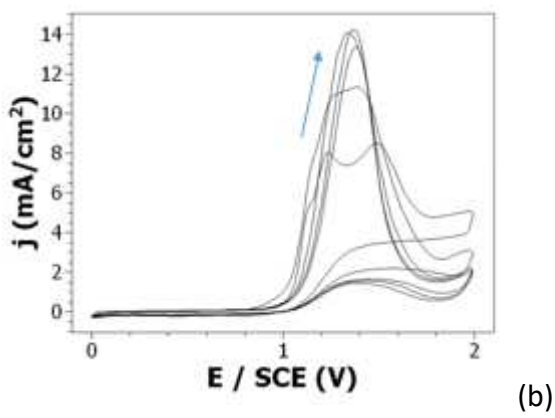

(b)

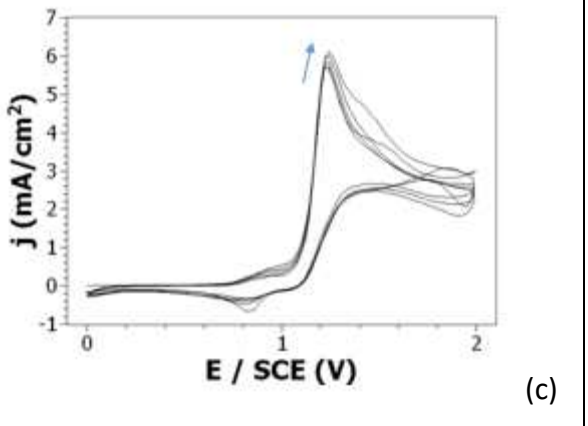

(c)

Figure 9: Cyclic voltammograms obtained at a Pt electrode from a: (a) Cz:CzE 50:50, (b) Cz:CzE 30:70, (c) Cz:CzE 5:95 acetonitrile + 0.1 M $LiClO_4$ solution. Scan rate of 50 mV/s.

- Physico-chemical properties:

AFM topography images clearly evidenced that the structures of Cz_{50}-CzE_{50} and Cz_{30}-CzE_{70} films were columnar (Fig. 10a-10c) and comparable to the structure of Cz_{90}-CzE_{10} and Cz_{70}-CzE_{30} films previously investigated (Fig. 6c-6e). On the contrary, the structure of the Cz_5-CzE_{95} film looked much more globular. Besides, if the maximum height of the Cz_{50}-CzE_{50} and Cz_{30}-CzE_{70} films was high (1.28 µm and 0.99 µm, respectively), the height of the Cz_5-CzE_{95} film was strongly lower with only 0.23 µm, confirming that the electropolymerization was difficult when performed from an electrolytic solution containing so much CzE monomers. The AFM force adhesion of each polymer film was also investigated and no strong difference was measured since the average adhesion value was 11 ± 3 nN for Cz_{50}-CzE_{50} film, 15 ± 3 nN for Cz_{30}-CzE_{70} film, and 14 ± 3 nN for Cz_5-CzE_{95} film (Fig. 10b-d-f). Besides, Young modulus measurements were performed for each polymer film (Suppl. File 2) leading to very high values (115 GPa for Cz_{50}-CzE_{50}, 46 GPa for Cz_{30}-CzE_{70}, and 65 GPa for Cz_5-CzE_{95}) compared with some of the previous polymer films (Cz_{90}-CzE_{10} and Cz_{70}-CzE_{30}) whose Young modulus was estimated to less than 10 GPa. Consequently, the stiffness of the polymer films containing a high portion of CzE was more similar to the one of the polymer film obtained from oxidation of CzE whose stiffness was 161 GPa.

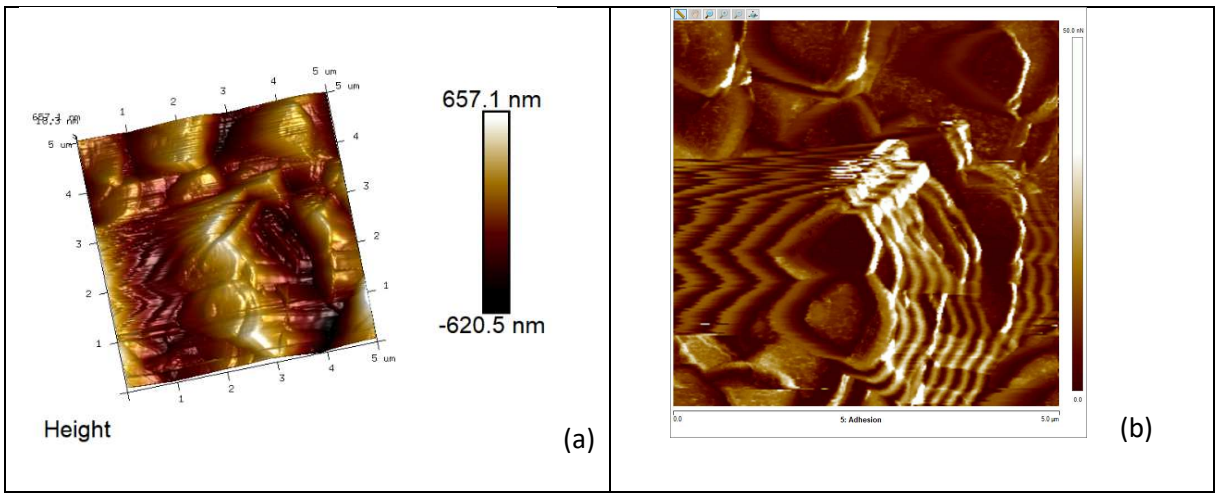

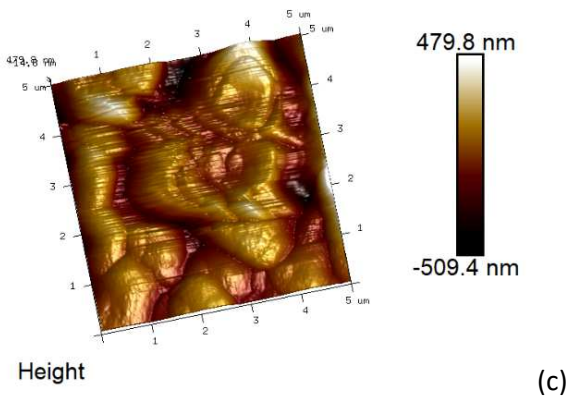

(c)

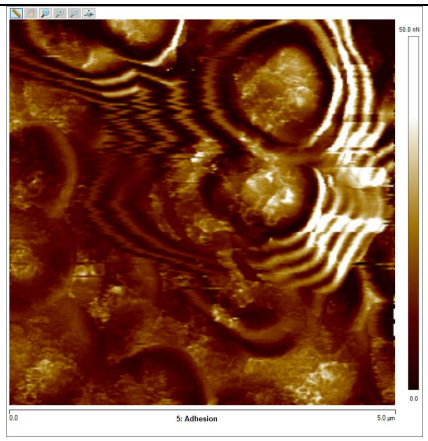

(d)

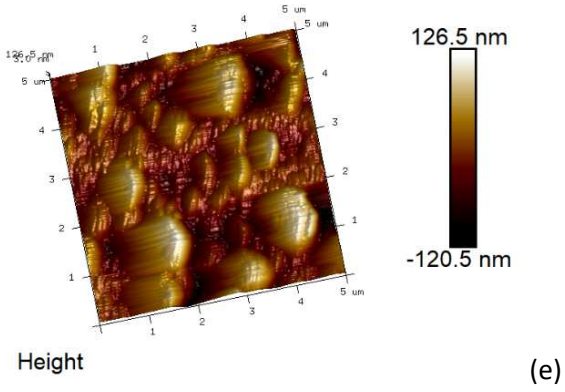

(e)

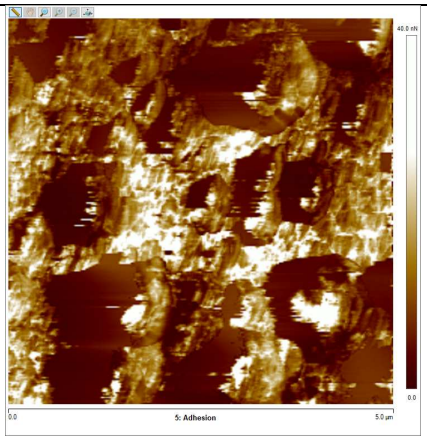

(f)

Figure 10: AFM topography (a,c,e) and adhesion images (b,d,f) of: Cz_{50}-CzE_{50} (a,b), Cz_{30}-CzE_{70} (c,d), and Cz_5-CzE_{95} (e,f) films.

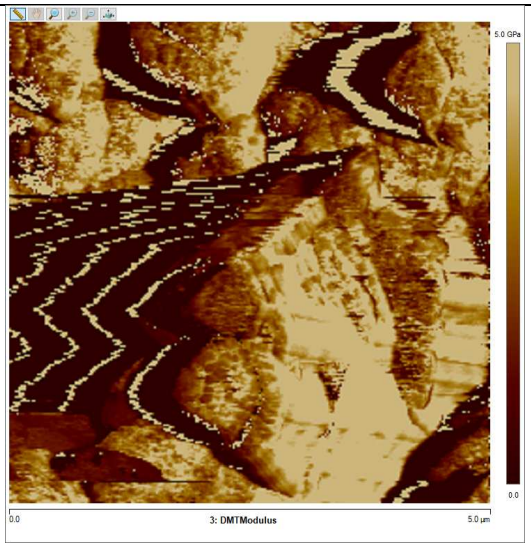

(a)

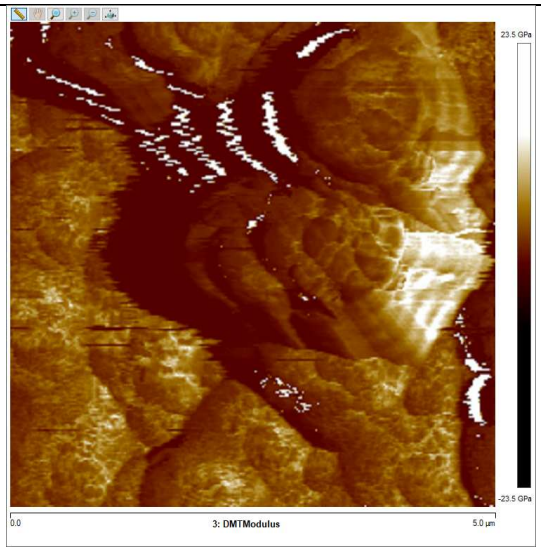

(b)

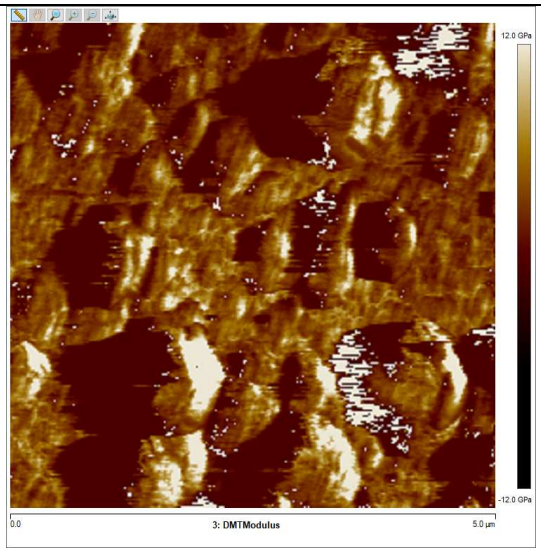

(c)

Supplementary File 2: AFM Young modulus measurements of: Cz_{50}-CzE_{50} (a), Cz_{30}-CzE_{70} (b), and Cz_5-CzE_{95} (c) films.

Table 2: Sum-up of the properties of the films obtained by oxidation of Cz, CzE and Cz:CzE mixtures (in green: beneficial properties, in red: adverse properties, in black: neutral properties).

	Aspect (naked-eye)	Young modulus (AFM)	Topography (AFM, SEM)	Intensity (CV)	Adhesion (AFM)	Height (AFM)	Insertion of ester groups
Cz	Green, Thick	High	Globular, Cracks	High	Medium	High	No
CzE	Colourless, Very thin	Very High	Globular	Medium	Medium	Very low	Yes
Cz_{95}-CzE_5	Green, Thick	Low	Globular, Cracks	High	Medium	High	Yes
Cz_{90}-CzE_{10}	Green, Thick	Very low	Columnar	High	Medium	High	Yes
Cz_{70}-CzE_{30}	Green, Thick	Very low	Columnar	High	Medium	High	Yes
Cz_{50}-CzE_{50}	Thin	Very High	Columnar	High	Medium	High	Yes
Cz_{30}-CzE_{70}	Thin	High	Columnar	High	Medium	High	Yes
Cz_5-CzE_{95}	Very thin	High	Globular	Medium	Medium	Low	Yes

4. Conclusion

The electrochemical polymerization of carbazole monomers with N-((methoxycarbonyl)methyl)carbazole monomers was successfully achieved using both potentiodynamic and potentiostatic techniques. It was shown that the Cz-CzE monomers ratio had a very significant impact on some physico-chemical properties of the electrodeposited films. In particular, depending on the Cz:CzE ratio introduced into the electrolytic solution, the morphology of the polymer film can be granular or columnar. Also, very wide Young's modulus variations were observed since they varied from 2 GPa for Cz_{70}-CzE_{30} to 115 GPa for Cz_{50}-CzE_{50}. This difference in stiffness is a key point since a high stiffness could be correlated with the presence of cracks in the polymer film while a low stiffness allowed the preparation of good quality films. So, it can be deduced from this study that the two most interesting polymer films are Cz_{70}-CzE_{30} and Cz_{90}-CzE_{10}. Indeed, these two polymer films are thick and dark green-coloured, present a good adhesion and a good electroactivity, contains ester groups, possess a low stiffness, exhibit an original columnar structure, and don’t contain any cracks.

Acknowledgments

This work was partly funded by the Bourgogne Franche-Comté Regional Council through the COMICS project. It was also supported by the french RENATECH network and its FEMTO-ST technological facility.

Figure Captions

Figure 1: Structure of carbazole (a) and N-((methoxycarbonyl)methyl)carbazole (b).

Figure 2: Cyclic voltammetry of 10^{-2} M Cz in 0.1 M $LiClO_4$/ACN at a Pt electrode with a scan rate of 50 mV/s (a). AFM (b) and SEM (c) images of the PCz film.

Figure 3: Photographs of samples deposited by oxidation of Cz, CzE and Cz:CzE mixtures.

Figure 4: Cyclic voltammetry of 10^{-2} M CzE in 0.1 M $LiClO_4$/ACN at a Pt electrode with a scan rate of 50 mV/s (a). AFM image of the PCzE film (b).

Figure 5: Cyclic voltammograms obtained at a Pt electrode from a: (a) Cz:CzE 95:5, (b) Cz:CzE 90:10, (c) Cz:CzE 70:30 acetonitrile + 0.1 M $LiClO_4$ solution. Scan rate of 50 mV/s.

Figure 6: Representations of the chemical structure (a), 3D orbitals (b), and 3D electron density (c) of 3,3'-CzCzE dimer (deduced from DFT calculations at the B3LYP/6-31G* level of theory).

Figure 7: AFM topography (a,c,e) and adhesion images (b,d,f) of: Cz_{95}-CzE_5 (a,b), Cz_{90}-CzE_{10} (c,d), and Cz_{70}-CzE_{30} (e,f) films.

Figure 8: SEM pictures of: Cz_{95}-CzE_5 (a), Cz_{90}-CzE_{10} (b), and Cz_{70}-CzE_{30} (c) films.

Figure 9: Cyclic voltammograms obtained at a Pt electrode from a: (a) Cz:CzE 50:50, (b) Cz:CzE 30:70, (c) Cz:CzE 5:95 acetonitrile + 0.1 M $LiClO_4$ solution. Scan rate of 50 mV/s.

Figure 10: AFM topography (a,c,e) and adhesion images (b,d,f) of: Cz_{50}-CzE_{50} (a,b), Cz_{30}-CzE_{70} (c,d), and Cz_5-CzE_{95} (e,f) films.

Table 1: Total free energy in solvent (in hartrees) of the different dimers that can be formed by coupling between Cz and CzE monomers.

Table 2: Sum-up of the properties of the films obtained by oxidation of Cz, CzE and Cz:CzE mixtures.

Supplementary File 1: AFM Young modulus measurements of: Cz_{95}-CzE_5 (a), Cz_{90}-CzE_{10} (b), and Cz_{70}-CzE_{30} (c) films.

Supplementary File 2: AFM Young modulus measurements of: Cz_{50}-CzE_{50} (a), Cz_{30}-CzE_{70} (b), and Cz_{5}-CzE_{95} (c) films.

References:

[1] H.G. Kiess, In: Conjugated conducting polymers, Springer-Verlag Berlin Heidelberg, Germany, 1992, 313 pp. 263-276.

[2] S. Kee, N. Kim, B. Park, B.S. Kim, S. Hong, J.H. Lee, S. Jeong, A. Kim, S.Y. Yang, K. Lee, Highly deformable and See-through Polymer Light-Emitting Diodes with All-Conducting-Polymer Electrodes, Advanced Materials 30 (2018) 1703437.

[3] S.A. Umoren, M.M. Solomon, Protective polymeric films for industrial substrates: a critical review on past and recent applications with conducting polymers and polymer composites/nanocomposites, PROG; Mater. Sci. 104 (2019) 380-450.

[4] H. Gao, K. Lian, Proton-conducting polymer electrolytes and their applications in solid supercapacitors: a review, RSC Advances 62 (2014) 33091-33113.

[5] M.A. Naveen, N.G. Gurudatt, Y.B. Shim, Applications of conducting polymer composites to electrochemical sensors: a review, Appl. Mater. Today 9 (2017) 419-433.

[6] B.T. Deepshikha, A review on Synthesis and Characterization of Nanostructured Conducting Polymers (NSCP) and Application in Biosensors, Anal. Lett. 44 (2011) 1126-1171.

[7] M. Talikowska, X. Fu, G. Lisak, Application of conducting polymers to wound care and skin tissue engineering: a review, Biosens. Bioelectron. 135 (2019) 50-63.

[8] T.P. Kaloni, P.K. Giesbrecht, G. Schreckenbach, M.S. Freund, Polythiophene: From Fundamental Perspectives to Applications, Chem. Mater. 29 (2017) 10248-10283.

[9] U. Mehmood, A. Al-Ahmed, I.A. Hussein, Review on recent advances in polythiophene based photovoltaic devices, Renew. Sust. Energy Rev. 57 (2016) 550-561.

[10] G. Liao, Q. Li, Z. Xu, The chemical modification of polyaniline with enhanced properties : a review, Progr. Org. Coat. 126 (2019) 35-43.

[11] N.K. Jangid, S. Jadoun, N. Kaur, A review on high-throughput synthesis, deposition of thin films and properties of polyaniline, Eur. Polym. J. 125 (2020) 109485.

[12] M.A. Chougule, Synthesis and characterization of polypyrrole (PPy) thin films, Soft Nanosci. Lette 1 (2011) 6-10.

[13] R. Jain, N. Jadon, A. Pawaiya, Polypyrrole based next generation electrochemical sensors and biosensors: a review, TRAC 97 (2017) 363-373.

[14] Q. Zhao, S.J. Liu, W. Huang, Polyfluorene-based blue-emitting materials, Macromol. Chem. Phys. 210 (2009) 1580-1590.

[15] Y.Y. Deng, H. Sirringhaus, Optical absorptions of polyfluorene transistors, Phys. Rev. B 72 (2005) 045207.

[16] Z. Rahimzadeh, S.M. Naghib, Y. Zare, K.Y. Rhee, An overview on the synthesis and recent applications of conducting poly(3,4-ethylenedioxythiophene) (PEDOT) in industry and biomedicine, J. Mater. Sci. 55 (2020) 7575-7611.

[17] M.N. Gueye, A. Carella, J. Faure-Vincent, R. Demadrille, J.P. Simonato, Progress in understanding structure and transport properties of PEDOT-based materials: A critical review, Prog. Mater. Sci. 108 (2020) 100616.

[18] Q. Chen, B.H. Han, Microporous Polycarbazole Materials: From Preparation and Properties to Applications, Macromol. Rapid Commun. 39 (2018) 1800040.

[19] S. Yapi Abe, J.C. Bernede, L. Ugalde, Y. Tregouet, M.A. del Valle, Electrochemical deposition of polycarbazole thin films onto tin oxide coated glass: physicochemical and optoelectronic characterizations, J. Appl. Polym. Sci. 106 (2007) 1568-1575.

[20] J.F. Morin, M. Leclerc, D. Ades, A. Siove, Polycarbazoles: 25 years of progress, Macromol. Rapid Commun. 26 (2005) 761-778.

[21] Y. Zou, D. Gendron, R. Badrou-Aïch, A. Najari, Y. Tao, M. Leclerc, A high-mobility low-bandgap poly(2,7-carbazole) derivative for photovoltaic applications, Macromolecules 42 (2009) 2891-2894.

[22] N. Blouin, A. Michaud, M. Leclerc, A low-bandgap poly(2,7-carbazole) derivative for use in high-performance solar cells, Adv. Mater. 19 (2007) 2295-2300.

[23] K. Karon, M. Lapkowski, Carbazole electrochemistry: a short review, J. Solid State Electrochem. 19 (2015) 2601-2610.

[24] K. Karon, M. Lapkowski, A. Dabuliene, A. Tomkeviciene, N. Kostiv, J.V. Grazulevicius, , Spectroelectrochemical characterization of conducting polymers from star-shaped carbazole-triphenylamine compounds, Electrochim. Acta 154 (2015) 119-127.

[25] P. Ledwon, P. Zassowski, T. Jarosz, Pashazadeh, M. Lapkowski, P. Wagner, V. Cherpak, P. Stakhira, A novel donor–acceptor carbazole and benzothiadiazole material for deep red and infrared emitting applications, J. Mater. Chem. C. 4 (2016) 2219-2227.

[26] G. Puckyte, B. Schmaltz, A. Tomkeviciene, M. Degbia, J.V. Grazulevicius, H. Melhem, J. Bouclé, F. Tran-Van, Carbazole-based molecular glasses for efficient solid-state dye-sensitized solar cells, J. Power Sources 233 (2013) 86-92.

[27] R. Pashazadeh, P. Pander, A. Lazauskas, F.B. Dias, J.V. Grazulevicius, Multicolor Luminescence Switching and Controllable Thermally Activated Delayed Fluorescence Turn

on/Turn off in Carbazole–Quinoxaline–Carbazole Triads, J. Phys. Chem. Lett. 9 (2018) 1172-1177.

[28] E. Sezer, B. Ustamehmetoglu, A. Sezai Sarac, Chemical and electrochemical polymerisation of pyrrole in the presence of N-substituted carbazoles, Synth. Met. 107 (1999) 7-17.

[29] T.A.P. Hai, R. Sugimoto, Conjugated carbazole-thiophene copolymer: Synthesis, characterization and applications, Synth. Met. 220 (2016) 59-71.

[30] J.A. Aristizabal, J.C. Ahumada, J.P. Soto, Electrochemical preparation and characterization of a new conducting copolymer of 2,7-carbazole and 3-octylthiophene, Polym. Bull. 74 (2017) 1649-1660.

[31] M. Guzel, T. Soganci, R. Ayranci, M. Ak M, Smart windows application of carbazole and triazine based star shaped architecture, Phys. Chem. Chem. Phys. 18 (2016) 21659-21667.

[32] M. Guzel, T. Soganci, M. Akgun, M. Ak, Carbazole functionalized star shaped triazine monomer and its electrochromic applications, J. Electrochem. Soc. 162 (2015) H527-H534.

[33] S. Li, X. Deng, L. Feng, X. Mia, K. Tang, Q. Li, Z. Li, Copolymers of carbazole and phenazine derivatives: minor structural modification, but totally different phtodetector performance, Polym. Chem. 8 (2017) 1039-1048.

[34] C. Yang, H.S. Song, D.B. Liu, Synthesis and properties of blue light electroluminescent conjugated copolymer based on fluorene and carbazole with an alkyl functional group at the 9-position, J. Mater. Chem. 47 (2012) 3315-3319.

[35] Q. Zou, F. Tao, H. Wu, W.W. Yu, T. Li, Y. Cui, A new carbazole-based colorimetric and fluorescent sensor with aggregation induced emission for detection of cyanide anion, Dyes Pigments 164 (2019) 165-173.

[36] W. Li, Y. Hu, Y. Song, Y. Gu, W. Wang, New carbazole fluorescent sensor for ultrasensitive and ratiometric sensing of SO_2 derivatives and hydrazine, J. Photochem. Photobiol. A 389 (2020) 112269.

[37] K. Kala, N. Manoj, A carbazole based “Turn on” fluorescent sensor for selective detection of Hg^{2+} in an aqueous medium, RSC Adv. 6 (2016) 22615-22619.

[38] X.J. Feng, P.Z. Tian, Z. Xu, S.F. Chen, M.S. Wong, Fluorescent-enhanced chemosensor for metal cation detection based on pyridine and carbazole, J. Org. Chem. 78 (2013) 11318-11325.

[39] R. Olgac, T. Soganci, Y. Baygu, Y. Gok, M. Ak, Zinc(II) phthalocyanine fused in peripheral positions octa-substituted with alkyl linked carbazole: Synthesis, electropolymerization and its electro-optic and biosensor applications, Biosens. Bioelectron. 98 (2017) 202-209.

[40] S. Cosnier, S. Szunerits, R.S. Marks, J.P. Lellouche, K. Perié, Mediated electrochemical detection of catechol by tyrosinase-based poly(dicarbazole) electrodes, J. Biochem. Biophys. Meth. 50 (2001) 65-77.

[41] K. Perie, R. Marks, S. Szumerits, S. Cosnier, J.P. Lellouche, Novel electro-oxidizable chiral N-substituted dicarbazoles and resulting electroactive films for covalent attachment of proteins, Tetrahedron Lett. 41 (2000) 3725-3729.

[42] E. Contal, C.M. Sougueh, S. Lakard, A. Et Taouil, C. Magnenet, B. Lakard, Investigation of Polycarbazoles Thin Films prepared by Electrochemical Oxidation of Synthesized Carbazole Derivatives, Frontiers Materials 6 (2019) 131.

[43] T.M. McCormick, C.R. Bridges, E.I. Carrera, P.M. DiCarmine, G.L. Gibson, J. Hollinger, L.M. Kozycz, D.S. Seferos, Conjugated Polymers: Evaluating DFT Methods for More Accurate Orbital Energy Modeling, Macromolecules 46 (2013) 3879-3886.

[44] W. Zhuang, M. Bolognesi, M. Seri, P. Henriksson, D. Gedefaw, R. Kroon, M. Jarvid, A. Lundin, E. Wang, M. Muccini, M.R. Andersson, Influence of Incorporating Different Electron-Rich Thiophene-Based Units on the Photovoltaic Properties of Isoindigo-Based Conjugated Polymers: An Experimental and DFT Study, Macromolecules 46 (2013) 8488-8499.

[45] I.H. Nayyar, E.R. Batista, S. Tretiak, A. Saxena, D.L. Smith, R.L. Martin, Localization of Electronic Excitations in Conjugated Polymers Studied by DFT, J. Phys. Chem. Lett. 2 (2011) 566-571.

[46] J.J.P. Stewart, Optimization of parameters for semiempirical methods I. Method, J. Comput. Chem. 10 (1989) 209-220.

[47] A.D. Becke, A new mixing of Hartree-Fock and local density-functional theories, J. Chem. Phys. 98 (1993) 1372–1377.

[48] C. Lee, W. Yang, R.G. Parr, Development of the Colle-Salvetti correlation-energy formula into a functional of the electron density, Phys. Rev. B. 37 (1988) 785-789.

[49] J.F. Ambrose, R.F. Nelson, Anodic oxidation pathways of carbazoles (I. Carbazole and N-substituted derivatives), J. Electrochem. Soc. 115 (1968) 1159-1163.

[50] R. Ravindranath, P.K. Ajikumar, S. Bahulayan, N.B. Hanafiah, A. Baba, R.C. Advincula, W. Knoll, S. Valiyaveettil, Ultrathin conjugated polymer network films of carbazole functionalized poly(p-phenylenes) via electropolymerization, J. Phys. Chem. B 111 (2007) 6336-6343.

[51] M. Lapkowski, J. Zak, K. Karon, B. Marciniec, W. Prukała, The mixed carbon–nitrogen conjugation in the carbazole based polymer; the electrochemical, UV Vis, EPR, and IR studies on 1,4-bis[(E)2-(9H-carbazol-9-yl)vinyl]benzene. Electrochim. Acta 56 (2011) 4105-4111.

Electrochemical preparation and physicochemical study of copolymers obtained from carbazole and N-((methoxycarbonyl)methyl)carbazole

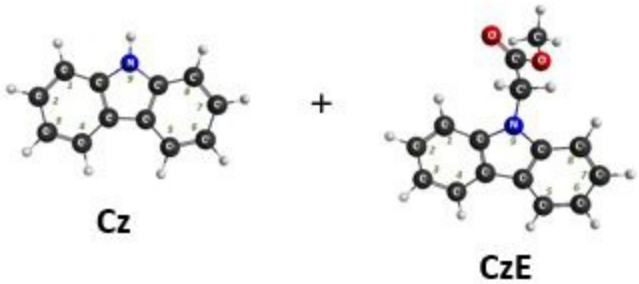

Best polymer films obtained from 90-10 and 70-30 Cz-CzE ratio:

Dark green thick coatings with granular structure and low Young modulus

90-10 Cz-CzE ratio

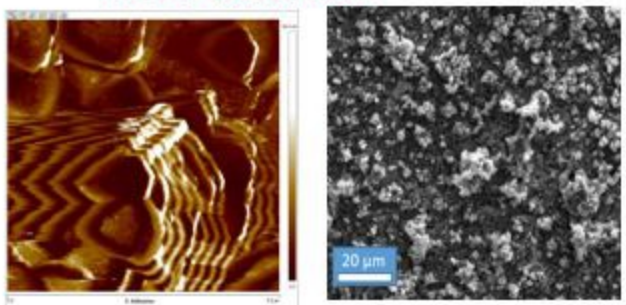

70-30 Cz-CzE ratio